Airborne Infection Isolation Room with Low-Cost Operating System

Nawee Nuntapap[1], Pracha Yeunyongkul[1,*], Jirasak Panya[1], Supachat Krudtong[1], Korawat Wuttikid[1], Thanawat Watcharadumrongsak[1], Srithorn Aupakham[1], Theerapat Boonsri[1], Parkpoom Jarupoom[2], Arpiruk Hokpunna[3], Nattaporn Chaiyat[4] and Ronnachart Munsin[1]

[1] Department of Mechanical Engineering, Rajamangala University of Technology Lanna, Huay Kaew Road, Muang, Chiang Mai 50300, Thailand
[2] Department of Industrial Engineering Faculty of Engineering, Rajamangala University of Technology Lanna, Huay Kaew Road, Muang, Chiang Mai 50300, Thailand
[3] Department of Mechanical Engineering, Faculty of Engineering, Chiang Mai University, Chiang Mai 50200, Thailand
[4] Thermal Design and Technology Laboratory (TDeT Lab), School of Renewable Energy, Maejo University, Nonghan, Sansai, Chiang Mai, 50290, Thailand

ypracha@rmutl.ac.th* (corresponding author)

Abstract. *The objective of this work is to develop an airborne infection isolation room (AIIR) with the air control system. The commercial sensors and the proportional integral derivative (PID) control were used in the control system. All sensors were calibrated before use for the system. User interface was developed by using LabVIEW. Key parameter for design of the control system was capability of pressure reduction, i.e. -2.5 Pa. Flow distribution in the AIIR with the variation of outlet position at 10, 60 and 100 cm height was also analyzed to find proper position. From design and development of the system, the tests showed that from the start of operation, the system with PID control decreased room pressure to each setpoint, i.e. -2.5, -4 and -6 Pa, in 15 seconds and maintained the pressure at the setpoint with stability. The outlet at 10 cm height showed low level of air dispersion and turbulence, while 60 cm height provided back flow and high dispersion of air.*

Received by 7 July 2022
Revised by 25 August 2022
Accepted by 9 October 2022

Keywords:

airborne infection isolation room, COVID-19, low-cost operating system, PID control

1. Introduction

The rapid spread of viral infectious diseases, Coronavirus Disease 2019 or COVID-19, occurred in a wide area around the world [1], including in Thailand. Medical resources preparation is essential to deal with this situation [2]–[5]. COVID-19 is a respiratory disease. It is necessary to separate the patient in a single negative-pressure room with one-way ventilation to prevent germs from the patient spreading to others. The ventilation principle in the room must not flow as a typical air-conditioned room. Usually, the negative pressure room for air infection patients is the single patient room with severe symptoms.

The pressure in the room can be controlled by the proportional integral derivative (PID) control if used closed loop control cannot control pressure. As shown in the previous works, PID controller and other techniques were applied to control the pressure of the sleep device. This control concept successfully balanced the pressure [6]. Li et al. [7] also showed that PID control can tackle the tuning parameters to improve the quality of indoor air. Other successful works using PID control are available in [8]–[11].

The negative-pressure rooms available in hospitals are still limited compared to the increasing of patients and the spread throughout the country. Therefore, it is important to prepare urgent medical facilities to accommodate these numbers of patients. Although the situation of Covid-19 epidemic has a tendency to reduce the number of infections at present and also Thailand has declared it as an endemic disease. But being prepared to add a negative pressure chamber is also very necessary [12], especially the development and construction of low-cost airborne isolation rooms. Therefore, this study aims to develop an airborne infection isolation room with the air control system.

2. Methodology

2.1 Sensor and Calibration

The available commercial sensors are used for a negative pressure room. The parameters from sensors need to be calibrated such as temperature, humidity and pressure. The sensor specifications have been shown by Table 1.

Sensor Specification			
Number	Features	Range	Accuracy
TMP36	Temperature Sensors	-40 to150°C	± 1 °C
AMT2001	Humidity Sensor	0~99 RH	± 0.5 %
XGZP164	Pressure Sensor	-1 to 1 kPa	± 0.3 Pa

Table 1 Sensor specification

These sensors were calibrated in the microclimate control room, where air temperature and relative humidity can be controlled separately. The calibrations of temperature and humidity had been conducted in 5 repetitions at level of confidence 95%. The Non-inverting Amplifier (IC Op amp LF353) was used to amplify the system with the gain of 8. The low-pass filter at 50 Hz was used to screen the error and noise.

In this research, the pressure difference between the isolate room and the ambient was measured. The pressure range of 0 – 10 Pascal was designed. The minimum value of negative pressure is at 2.5 Pa. To design the low-pressure measurement, the technique of inclined manometer at 1:10 degree is sin (9^o) has been applied as shown in Fig. 1. Water temperature is at 25 °C and density of 997 kg/m^3. Pressure was calculated by equation (1):

$$\Delta P = \rho\, g\, \sin(\theta)\, \Delta h \qquad (1)$$

From the sensor calibrations of temperature, humidity and pressure, the relationship between these three parameters and voltage are along the linear equation of $y = ax + b$. The equations are used with LabVIEW program to display on a computer and control the room.

2.2 Experimental Setup

This work is to design and build an automatic air control system in a negative pressure room. The prototype will be applied to the fieldwork negative pressure room. The design was based on studies in a variety of operating conditions. The parameters or experimental conditions will be adjusted in accordance with the characteristics of Thailand weather conditions. In addition, production costs, operating costs, maintenance costs, and energy costs will be analyzed together with the performance of the prototype for the possibility of further use in the industrial sector.

For the pressure control principle, inlet air blower was set at a constant speed. Flow and pressure inside the room was controlled by adjusting the speed of outlet air blower. In order to obtain an additional rate of outside air in the range over 12ACH and the pressure inside the room is negative less than 2.5 Pa or the specified value, the outlet air blower was controlled. It was relied on the air flow sensor F2 and the pressure sensor P1 which measure the difference pressure between the atmospheric pressure and the pressure inside the room. The signals were sent to the controller C2, data acquisition D1 and to computer to be calculated. The computed data sent signals back to data acquisition D1 and controller C2 to adjust the speed of motor at C4 according to the settings on the computer as shown in Fig. 2.

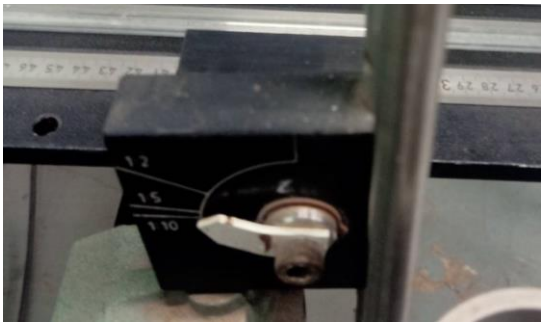

Fig. 1 Inclined manometer at 1:10 degree

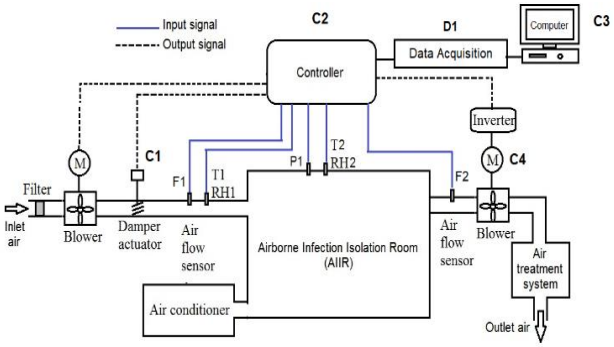

Fig. 2 Measurement and control system design.

To design and construction control system, control commands will be programmed. Proportional Integral Derivative Control (PID) was used to display and control the pressure value to be in accordance with the specified values and in accordance with the standards [10]. The advantage of PID control is that system will adjust the error of the controlled value to be close to the desired value by relying on the results feedback of the data until a stable control value is obtained. This makes PID control more accurate and stable as shown in Fig. 3. The system is displayed and can be controlled at the computer screen as shown in Fig. 4. Pressure, temperature and humidity information are displayed and recorded. It has capable to adjust the pressure, air condition and lighting control. Experimental conditions at -2.5 to -6 Pa with adjustment of K_c, Ti and Td as shown in ผิดพลาด! ไม่พบแหล่งการอ้างอิง.

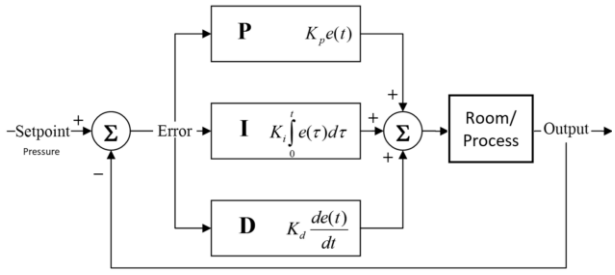

Fig. 3 Pressure setting conditions with PID control.

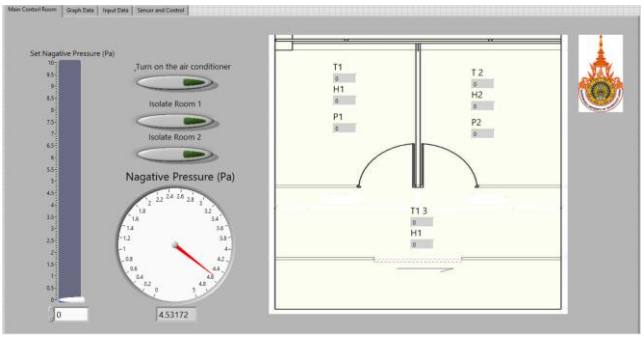

Fig. 4 User interface.

Parameter		Value
Pressure (Pa)		-2.5, -4, -6
PID setting condition	K_c	1, 1.4
	T_i	0.01, 0.015
	T_d	0.001

Table 2 Experimental Condition

2.3 Air Flow Simulation in the AIIR

Computational fluid dynamics (CFD) was used to analyze flow pattern in the AIIR to find the proper position of the outlet. In this work, the proper position of the outlet was studied by changing the height from 10, 60 and 100 cm above the floor, while the inlet was kept at a position on the ceiling. The position of outlet was on the wall behind the patient. However, the model of patients and bed were not put in simulation because this work focused on the control system. The model of patients and bed are considered in the future works. The dimension of model is 2.44 m width × 3.27 m length × 2.77 m height as shown in Fig. 5 and the boundary conditions as shown in Table 3.

Inlet	Outlet
Duct sizing 0.9 m^2	Duct sizing 1.2 m^2
Cartesian (X,Y,Z)	Fixed Pressure
U = 0 m/s, V = 3 m/s ,W = 0 m/s	Gauge Pressure = 0
T= 300 K	T =300K
Standard k-ε	Standard k-ε

Table 3 Boundary conditions

The governing equations used are shown in equation (2) to (4):

$$\frac{\partial \rho}{\partial t} + \nabla \cdot (\rho \boldsymbol{v}) = 0 \quad (2)$$

$$\frac{\partial}{\partial t}(\rho \boldsymbol{v}) + \nabla \cdot (\rho \boldsymbol{v}\boldsymbol{v}) = -\nabla p + \nabla \cdot (\boldsymbol{\tau}) + \rho \boldsymbol{g} + \boldsymbol{F} \quad (3)$$

$$\frac{\partial}{\partial t}(\rho E) + \nabla \cdot \left(\boldsymbol{v}(\rho E + p)\right) = \nabla \cdot \left(k_{eff} \nabla T\right) + S_h \quad (4)$$

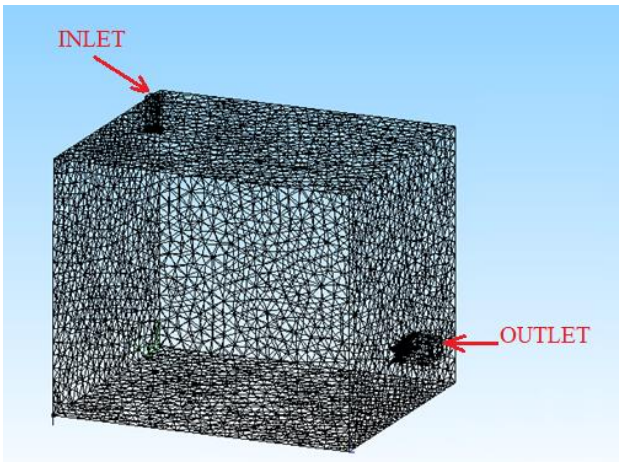

Fig. 5 Model of the airborne infection isolation room for simulation.

Where ρ, t, $\boldsymbol{v}$, p, $\boldsymbol{\tau}$, $\boldsymbol{g}$, $\boldsymbol{F}$, E, k_{eff}, T and S_h are density, time, flow velocity, pressure, stress tensor, gravity, momentum sink term, total energy, effective conductivity, temperature and volumetric heat source, respectively. The assumption referred to [13] to reduce the calculation complexity. The flow in AIIR was steady, incompressible flow and no slip wall condition. The inlet velocity used for simulation was 0.25 m/s with the turbulence intensity of 2%. The atmospheric pressure was assigned for the outlet. The convergence criterion is the residual error of variables less than 0.0001. The iteration number was 5,000 cycles. For illustration, the center room-cut plane showing in Fig. 6 was used to represent air flow in the AIIR.

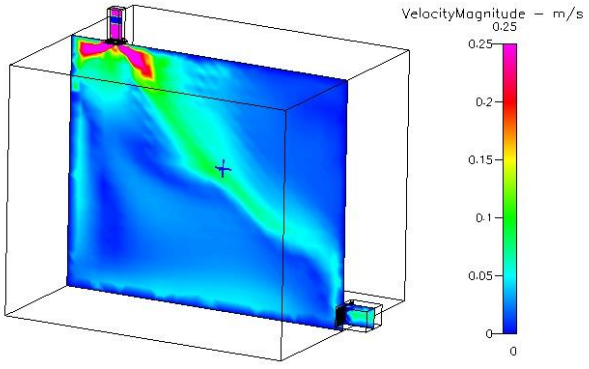

Fig. 6 The plane for illustration at the center of the AIIR.

As shown in the figure of flow distribution, the velocity at the inlet and outlet was different, because of the difference of flow area. However, the flow rates at the inlet and outlet are similar with the residual error less than the order of 10-6 kg/s as shown in the mass flow summary below shown in Fig. 7.

```
 Boundary-by-Boundary Mass Flow Summary (kg/sec)
 ================================================================================
       Name              Key  Type        Inflow         Outflow        Sum
 ================================================================================
FACE_2                    3  Outlet      0.00000E+00  -9.93021E-02  -9.93021E-02
FACE_15                  16  Inlet       9.92997E-02   0.00000E+00   9.92997E-02
 --------------------------------------------------------------------------------
 Total volume source                                                  0.00000E+00
 --------------------------------------------------------------------------------
 --------------------------------------------------------------------------------
 Total Mass Flow Summary                 9.92997E-02  -9.93021E-02  -2.41048E-06
 ================================================================================

 ====================================
 Current Iteration # :         1975
 ====================================
 ================================================================================
  Boundary-by-Boundary Mass Flow Summary (kg/sec)
 ================================================================================
       Name              Key  Type        Inflow         Outflow        Sum
 ================================================================================
FACE_2                    3  Outlet      0.00000E+00  -9.93013E-02  -9.93013E-02
FACE_15                  16  Inlet       9.92997E-02   0.00000E+00   9.92997E-02
 --------------------------------------------------------------------------------
 Total volume source                                                  0.00000E+00
 --------------------------------------------------------------------------------
 --------------------------------------------------------------------------------
 Total Mass Flow Summary                 9.92997E-02  -9.93013E-02  -1.59316E-06
 ================================================================================

 ====================================
 Current Iteration # :         2000
 ====================================
 ================================================================================
  Boundary-by-Boundary Mass Flow Summary (kg/sec)
 ================================================================================
       Name              Key  Type        Inflow         Outflow        Sum
 ================================================================================
FACE_2                    3  Outlet      0.00000E+00  -9.93008E-02  -9.93008E-02
FACE_15                  16  Inlet       9.92997E-02   0.00000E+00   9.92997E-02
 --------------------------------------------------------------------------------
 Total volume source                                                  0.00000E+00
 --------------------------------------------------------------------------------
 --------------------------------------------------------------------------------
 Total Mass Flow Summary                 9.92997E-02  -9.93008E-02  -1.07226E-06
 ================================================================================


  ============================
  End   of Iterative Cycle.....
  ============================

       Final Time   Elapsed Time=  5.762500E+01 Delta-time=  5.762500E+01

 Normal Termination
```

Fig. 7 The mass flow summary below

3. Results and Discussion

3.1 Calibration of Sensors

The results of temperature sensor calibration (TMP36) are shown in Fig. . The Non-inverting Amplifier, IC Op amp LF353, was used with the gain of 8. The low-pass filter, 50 Hz, was used to measure the error and noise; including the linear equation, confidence value and error of measurement.

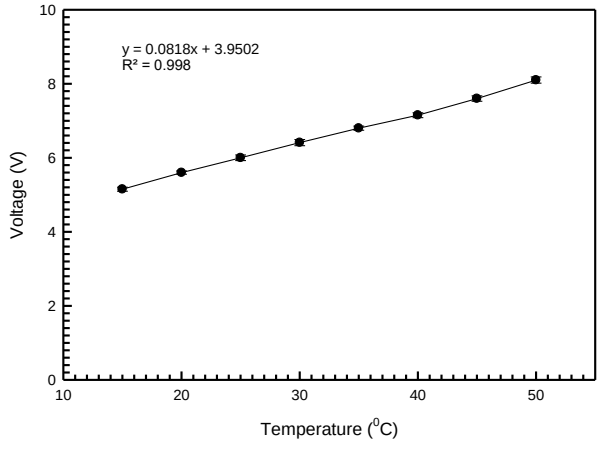

Fig. 8 Comparison of voltage and temperature sensor tmp36 at humidity 60%

The humidity calibration at temperature of 25 °C is shown in Fig. 9. The signal was amplified with the gain of 3 and filtered through the 50 Hz low-pass filter.

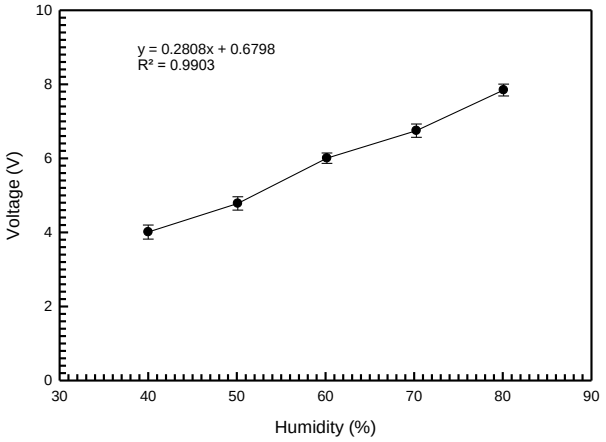

Fig. 9 Comparison of voltage and humidity sensor AMT2001 at 25°C

Since the negative pressure was low, the pressure measurement was designed at most 10 Pa by IC Instrumentation Amplifiers INA129 as shown in Fig.10. The Signal amplifying with the gain of 5,000 and the low-pass filter, 50 Hz, were used.

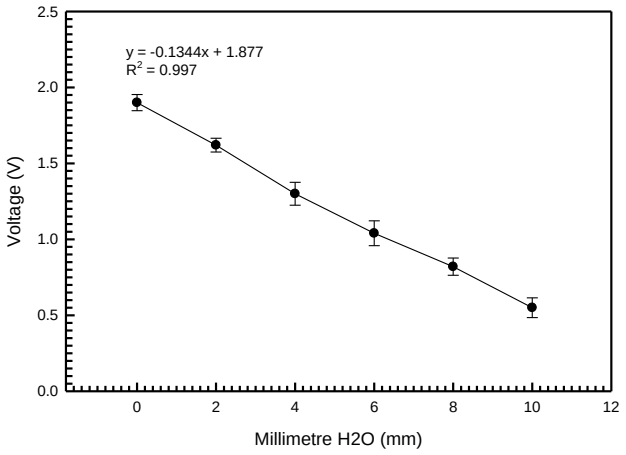

Fig. 10 Comparison of voltage and water difference

From the experimental results, it was found that when the pressure was adjusted at -2.5 to -6 pa and also adjusted Kc = 1, Ti = 0.01 and Td = 0.001 by LabVIEW. The overshoot and undershoot had occurred along the pressure range at 6 to 12 second respectively before entering the set pressure. when changed the values to Kc = 1.4, Ti = 0.015 and Td = 0.001, entering the set pressure did not show the overshoot or overshoot. That means the Kc and Ti values effect the convergence as shown in 11.

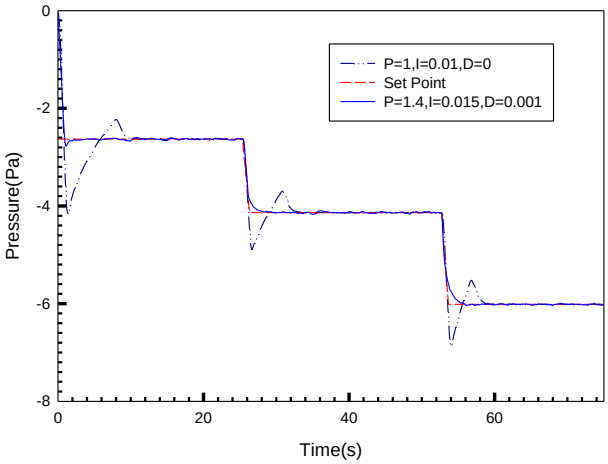

Fig. 7 Pressure on step response

3.2 Effect of Outlet Position on Flow Pattern in AIIR

Flow distribution change due to the position of outlet is shown in Fig.12. As expected, it is clear that the difference of outlet position resulted in flow pattern. Air stream from the inlet can partially move to the outlet in case of outlet height of 10 and 60 cm in Fig. (a) and (b), respectively. The direction of flow will pass the position of patient head (around 60 cm height and near the right wall). The outlet at 10 cm height provided downward flow and move out of the room which is good to control germ dispersion, while air stream in case of the outlet at 60 cm height hit the corner of the room and move backward along the floor air resulting in swirl near to the opposite wall. For outlet height of 100 cm, air was highly dispersed to everywhere in the room with backward pattern. This was worst for the AIIR because it is possible that germ from the patient and the floor can be dispersed by high dispersion of air. From the simulation, the outlet at 10 cm height was recommended for this work. Flow distribution in the AIIR y-cut as shown in Fig.13(a)-(c).

4. Conclusion

PID control was applied to the control system. Low-cost operating system can reduce the room pressure as low as -6 Pa. For the operations, the control system successfully maintained room pressure at the desired setpoint. The outlet at 10 cm height was recommended for the AIIR to reduce the air dispersion in the room.

The future works extending from this work were planned. The first work will focus on the control system with low-cost operating system for multiple AIIRs, followed by the system parametric study to enhance the performance and the energy efficiency of the system. In addition, flow analysis with the complexity of the model, including patients, doctor or nurse and objects in the room, will be considered.

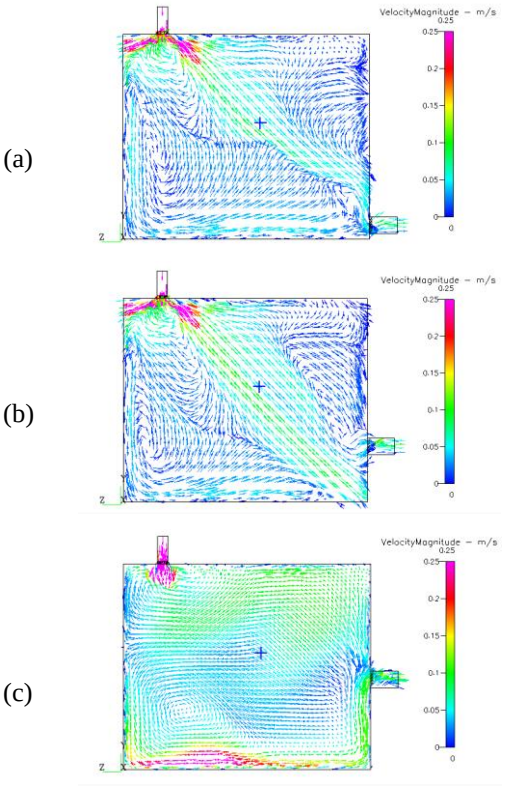

Fig. 12 Flow distribution in the AIIR x-cut at outlet height of (a) 10 cm, (b) 60 cm and (c) 100 cm.

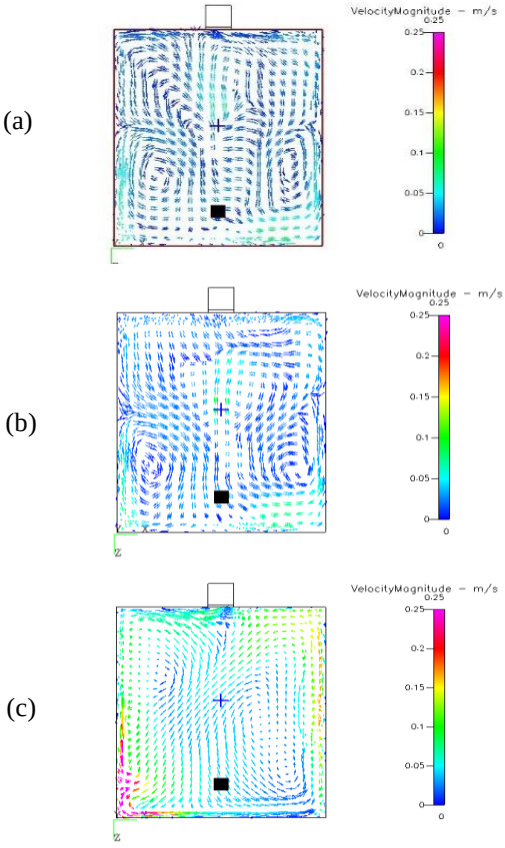

Fig. 13 Flow distribution in the AIIR y-cut at outlet height of (a) 10 cm, (b) 60 cm and (c) 100 cm.

Acknowledgements

The financial support of this work was provided by the Thailand Science Research and Innovation (TSRI) through the fundamental fund 2022. The authors acknowledge the project supported by the National Research Council of Thailand (NRCT) through the research and innovation grant (No.N25A650020) for providing the simulated microclimate and for the sensor calibration. The authors also express the sincere gratitude to Mr.Nopphadon Jongboon and Mr.Satit Karnpian for their helps during experiments.

References

[1] "International cooperation for the coronavirus combat results, lessons, and Way Ahead," http://pl.chinaembassy.gov.cn/pol/zt/FNCV/202003/t20200310_2370533.htm (accessed Jul. 07, 2022).

[2] J. K. Lee and H. W. Jeong, "Rapid expansion of temporary, reliable airborne-infection isolation rooms with negative air machines for critical COVID-19 patients, " *Am. J. Infect. Control*, vol. 48, no. 7, pp. 822–824, Jul. 2020, doi: 10.1016/j.ajic.2020.04.022.

[3] B. desu, L. Tilahun, and M. Zeleke, "Preparedness of governmental hospitals for COVID 19 prevention and care in Eastern Amhara region, Amhara Ethiopia, 2020," *Heart Lung*, pp. S0147956322001509, Jun. 2022, doi: 10.1016/j.hrtlng.2022.06.017.

[4] K. Skok *et al.*, "COVID-19 autopsies: Procedure, technical aspects and cause of fatal course. Experiences from a single-center," *Pathol. - Res. Pract.*, vol. 217, pp. 153305, Jan. 2021, doi: 10.1016/j.prp.2020.153305.

[5] F. Ventura, A. Molinelli, and R. Barranco, "COVID-19-related deaths in residential care homes for elderly: The situation in Italy," *J. Forensic Leg. Med.*, vol. 80, pp. 102179, May 2021, doi: 10.1016/j.jflm.2021.102179.

[6] A. Golcuk, "Design and implementation of a hybrid FLC + PID controller for pressure control of sleep devices, " *Biomed. Signal Process. Control*, vol. 76, pp. 103702, Jul. 2022, doi: 10.1016/j.bspc.2022.103702.

[7] S. Li, M. Wei, Y. Wei, Z. Wu, X. Han, and R. Yang, "A fractional order PID controller using MACOA for indoor temperature in air-conditioning room," *J. Build. Eng.*, vol. 44, pp. 103295, Dec. 2021, doi: 10.1016/j.jobe.2021.103295.

[8] A. Ferrari, A. Mittica, P. Pizzo, and Z. Jin, "PID Controller Modelling and Optimization in Cr Systems with Standard and Reduced Accumulators," *Int. J. Automot. Technol.*, vol. 19, no. 5, pp. 771–781, Oct. 2018, doi: 10.1007/s12239-018-0074-4.

[9] T.-Y. Guo, L.-S. Lu, S.-Y. Lin, and C. Hwang, "Design of maximum-stability PID controllers for LTI systems based on a stabilizing-set construction method," *J. Taiwan Inst. Chem. Eng.*, vol. 135, pp. 104366, Jun. 2022, doi: 10.1016/j.jtice.2022.104366.

[10] J. Liu and G. X. Wang, "The Optimization of Adaptive PID Control Algorithm Based on RBF Neural Network," *Adv. Mater. Res.*, vol. 998–999, pp. 943–946, Jul. 2014, doi: 10.4028/www.scientific.net/AMR.998-999.943.

[11] Ming-guang Zhang, Xing-gui Wang, and Man-qiang Liu, "Adaptive PID control based on RBF neural network identification," in *17th IEEE International Conference on Tools with Artificial Intelligence (ICTAI'05)*, Hong Kong, China, 2005, p. 3 pp.683. doi: 10.1109/ICTAI.2005.26.

[12] A. Mersha *et al.*, "Health professionals practice and associated factors towards precautionary measures for COVID-19 pandemic in public health facilities of Gamo zone, southern Ethiopia: A cross-sectional study," *PLOS ONE*, vol. 16, no. 3, pp. e0248272, Mar. 2021, doi: 10.1371/journal.pone.0248272.

[13] Manop Rakyat *et al.*, "Study of air distribution in tray dryer using computational fluid dynamics," *Eng. Appl. Sci. Res.*, vol. 48, pp. 684693, 2021, doi: 10.14456/EASR.2021.69.

Biographies

Nawee Nuntapap received his M.Eng. in Mechanical engineering from KMUTT, Thailand, in 2014. He is currently an assistant professor at Rajamangala University of Technology Lanna, Thailand. His research interests include measurement and instrumentation and control.

Pracha Yeunyongkul received his D.Eng. in Mechanical engineering from Chiang Mai University, Thailand, in 2012. He is currently an assistant professor at Rajamangala University of Technology Lanna, Thailand. His research interests include application of heat pipe, heat exchanger design and geopolymer.

Jirasak Panya received the M.Eng. in Mechanical Engineering from Chiang Mai University, Thailand, in 2009. He is currently a lecturer at the Department of Mechanical Engineering, Rajamangala University of Technology Lanna, Thailand. His research interests include machine design, refrigeration and air conditioning and fluid machinery.

Supachat Krudthong received the M.Eng. in Mechanical Engineering from Chiang Mai University, Thailand, in 2007. He is currently a lecturer at the Department of Mechanical Engineering, Rajamangala University of Technology Lanna, Thailand. His research interests focus on engineering mechanics, finite element and biomedical engineering.

Korawat Wuttikid is working as an instructor at Rajamangala University of Technology Lanna. He received bachelor, master and doctor degree in Mechanical Engineering from Chiang Mai University. His research focus on machine design for solving

Thanawat Watcharadumrongsak is working as an instructor at Rajamangala University of Technology Lanna, Thailand. He received doctor degree in Mechanical Engineering from Chiang Mai University, Thailand. His research focuses on heat transfer and applications.

Srithorn Aupakham is working as an instructor at Rajamangala University of Technology Lanna, Thailand. He received master degree in Mechanical Engineering from Chiang Mai University, Thailand. His research focuses on energy and air conditioning.

Theerapat Boonsri is a second-year master student under the supervision of Dr.Ronnachart Munsin. His current research focuses on ventilation within airborne infection isolation room.

Parkpoom Jarupoom received his Ph.D. in Materials Science from Chiang Mai University, Thailand, in 2011. He is currently an assistant professor at Rajamangala University of Technology Lanna, Thailand. His research interests include ceramic materials, biomaterials nanotechnology and manufacturing process.

Arpiruk Hokpunna received his doctorate in Engineering from the Technical University of Munich, Germany, in 2009. He is currently an assistant professor at Chiang Mai University, Thailand. His research field includes numerical methods for fluid flow, industrial modeling, simulation and design as well precision agriculture.

Nattaporn Chaiyat is working as an associate professor at Maejo University, Thailand. He received his D.Eng. in Energy Engineering from Chiang Mai University, Thailand, in 2011. His research interests focus on energy and renewable engineering.

Ronnachart Munsin is working as an assistant professor at RMUTL. He received his D.Eng. in Mechanical Engineering from KMUTT, Thailand, in 2015 and worked as a postdoctoral fellow at the Université d' Orléans, France, in 2016. His research focuses on atmospheric water harvesting, agricultural engineering and combustion.